International Journal of Power Electronics and Drive Systems (IJPEDS)
Vol. 14, No. 1, March 2023, pp. 100~110
ISSN: 2088-8694, DOI: 10.11591/ijpeds.v14.i1.pp100-110

Performances of a wind power system based on the doubly fed induction generator controlled by a multi-level inverter

Mohamed Salah Djebbar, Aziz Boukadoum, Abla Bouguerne
Department of Electrical Engineering, Faculty of Engineering Sciences, Larbi Tebessi University, Tebessa, Algeria

Article Info

Article history:

Received Jan 9, 2022
Revised Oct 27, 2022
Accepted Nov 11, 2022

Keywords:

Doubly fed induction generator
Indirect field-oriented control
Multi-level inverter
Pulse width modulation
Total harmonic distortion

ABSTRACT

The objective of this work is to study the contribution that the use of the multi-level inverter can make compared to a conventional two-level inverter, in a wind power production line (WPG) associated with a doubly fed induction generator (DFIG). The DFIG is driven by a variable speed wind turbine and operates in maximum power point tracking (MPPT) mode, for optimum efficiency. The rotor of the DFIG is supplied by a DC/AC inverter with five levels with MPC structure, controlled by the PWM technique, while the stator is connected with the network. The active and reactive powers exchanged between the DFIG and the network is achieved by indirect vector control with oriented stator flux (IFOC), with conventional regulators, ensuring zero reactive power and a unitary power factor. The total harmonic distortion (THD) of the current signals/voltages of the entire wind chain is exposed and criticized. The obtained results are very promising, offering the possibility for wind turbines with multi-level inverter to work in high voltage and large power.

Corresponding Author:

Mohamed Salah Djebbar
Department of Electrical Engineering, Faculty of Engineering Sciences, University Larbi Tebessi
Constantine Road, Tebessa12002, Algeria
Email: djebbarcn@yahoo.fr

1. INTRODUCTION

Wind power is a relatively large and constantly evolving field. Over the past decades, wind power has become the fastest growing renewable energy source in the world. It has known for about 30 years an unprecedented boom due in particular to the 1974 oil crisis [1]. This energy is clean and non-polluting, it doesn't emit any greenhouse gas, and its raw material, the wind, is available everywhere in the world and completely free [2]–[6]. Today, most wind turbines are equipped with a doubly fed induction generator (DFIG), associated with a static AC/DC/AC converter, to extract kinetic energy from the wind and convert it into electrical energy [7]. Indeed, this latter (DFIG) has several advantages, in particular: a better use of wind energy, the reduction of torque oscillations, a great reliability and a great flexibility in the connection to the network due to the use of power electronics converters [7].

The AC/D/AC converter is installed between the rotor of the DFIG and the electrical network in order to control the rotation speed of the turbine and therefore the generated power [8]–[10].The main objective of this work is to improve the research in the context of the production of electric energy by a wind conversion system and to evaluate the performance of the wind generator based on the doubly fed induction generator (DFIG), connected to the electrical network and integrated into the distribution network as shown in Figure 1.

The DFIG is supplied to the stator by a three-phase voltage source and the rotor by a two-level then five-level voltage inverter MPC structure, controlled by the technique of pulse width modulation (PWM).The operation of the DFIG is based on Indirect field oriented control (IFOC), with oriented stator flux, the purpose

of which is to decouple the active and reactive powers generated by the stator from the generator [11]–[13]. Closed-loop active and reactive power regulation is provided by integral proportional controllers (PI). The contribution made by the use of multi-level converters to our wind energy conversion system is evaluated at the end of this work, by the THD of the voltage/current wave at the rotor and stator of the machine (DFIG).

2. RESEARCH METHOD

Given the positive impact of the multi-level inverter on improving the quality of electrical signals (currents/voltages), by generating low harmonic distortion rates and the possibility of this type of converter to work under high voltages, compared to the conventional two-level inverter. It is in this vision that we proposed our work, which consists of the use of a five-level inverter in a wind energy production chain. Therefore, our work procedure consists in implementing in the first place, a two-level inverter and seeing the contribution that the latter can bring to the quality of the electrical energy in a wind energy production line (WPG), combined with a doubly fed induction generator (DFIG). Second, replace the two-level inverter with a five-level inverter in the same wind energy production chain and see the impact of the latter on the quality of the electrical signals (THD voltages/currents), in comparing its results obtained with those obtained by a two-level inverter.

The work methodology is also developed with the aim of highlighting the possibility of inserting multi-level inverters in a wind energy production line when it is to be worked under high voltages and high-power ranges. Since the latter offer the possibility of increasing the voltage in the DC bus, each time the structure (the topology) of the inverter takes a higher level (2 level, 3 level, and 5 level). This work aims only and essentially at the contribution of the multi-level inverter to the reduction of harmonic currents and harmonic voltages at the stator/rotor of the doubly fed induction generator in a low-voltage wind energy production chain.

3. WIND TURBINE MODELING AND CONTROL

3.1. Modeling of the wind turbine

Figure 1 represents the block diagram of the wind energy production chain based on the dual fed induction generator (DFIG), associated with a DC/AC converter, and connected to the electrical network. The exerted torque by the wind on the turbine shaft can be deduced directly from (1) by dividing the expression of the mechanical power by the speed of rotation of the engine shaft [14]–[18].

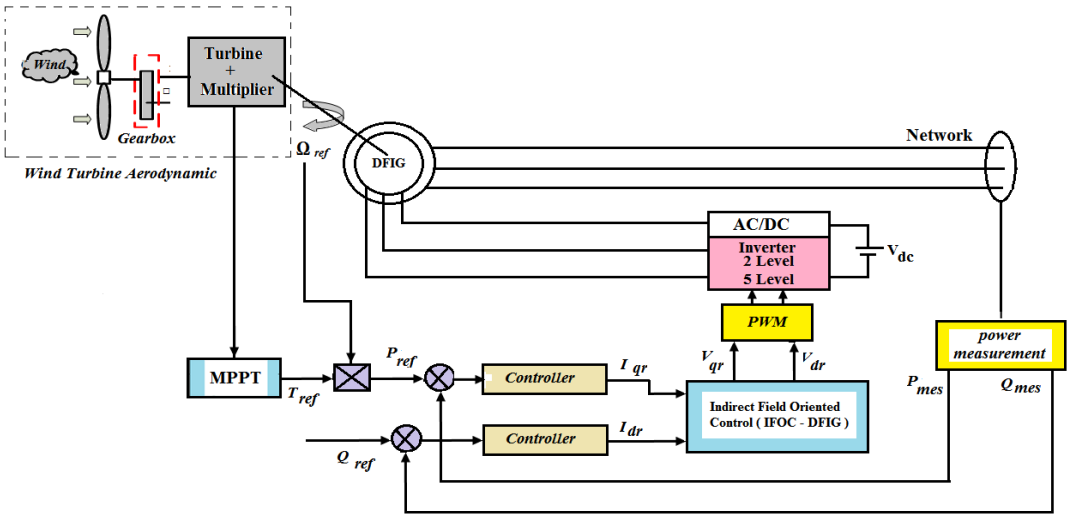

Figure 1. The block diagram of a wind system

The (1), gives the value of the wind torque, created on the turbine shaft by the mass of air having a speed.

$$T_{turb} = \frac{P_{aero}}{\Omega_{turb}} = \frac{1}{2\Omega_{turb}} C_p(\lambda)\rho\pi R^2 W_s^3 \quad (1)$$

With: R the radius of the wind turbine blades, ρ the density of the air (1.25 kg/m^3) and W_s the wind speed, Cp the Betz power coefficient. Knowing that λ is the speed ratio such that:

$$\lambda = \frac{R\Omega_t}{W_s} \tag{2}$$

Ω_t : The angular speed of the rotation of the wind turbine.
β : Wind turbine blade pitch angle, expressed in degrees.

The fundamental mechanical equation of the system on the electrical generator side is giving by (3) [19], [20].

$$\frac{T_{turb}}{G} - T_{DFIG} - f\Omega_{mec} = \left(\frac{J_{turb}}{G^2} + J_{DFIG}\right)\frac{d\Omega_{mec}}{dt} \tag{3}$$

The overall model of the turbine is illustrated in Figure 2.
Where:
T_{turb} is the wind turbine torque;
T_{DFIG} is the DFIG torque (load torque for the wind turbine);
f is the viscous friction;
G is the gearbox ratio.

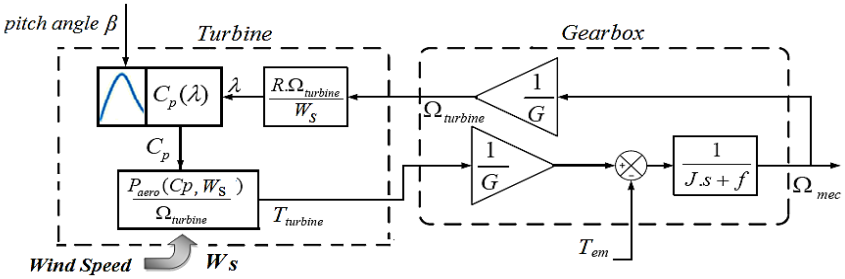

Figure 2. Overall diagram of the wind turbine

3.2. Wind turbine simulation

The used parameters of the wind turbine [21]; number of blades=3; radius of the surface swept by the blades: R=3m; multiplier gain: G=28; moment of inertia of the turbine J=315 kg.m²; viscous coefficient of friction: f=0.0024 N.m.s/rd. The wind profile appears in Figure 3(a), with an average value of (8 m/s) applied to the wind turbine. The power coefficient Cp, the blade pitch angle β and the relative speed ratio λ are shown in Figure 3(b), Figure 3(c) and Figure 3(d), respectively.

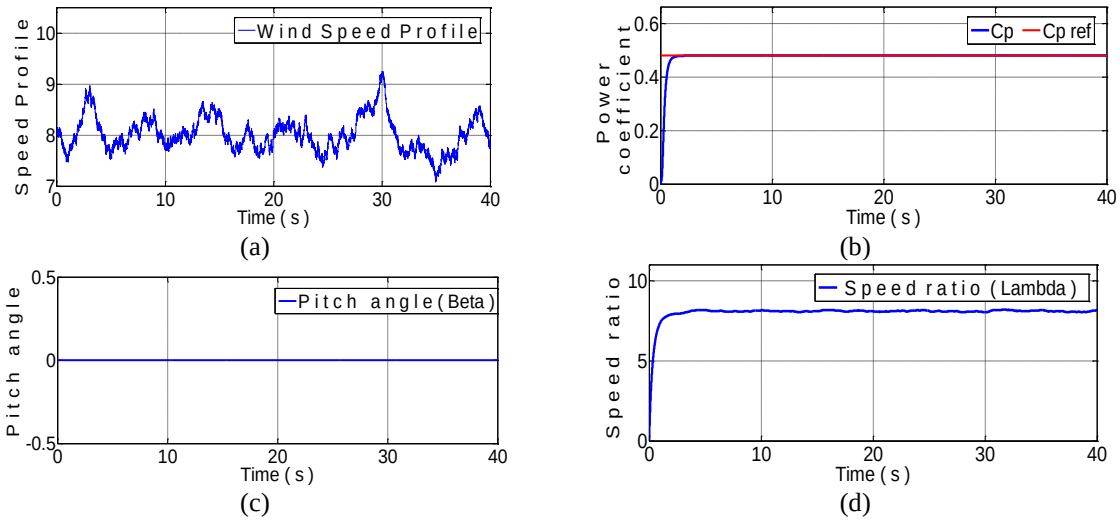

Figure 3. Wind profile (a) associated with the (b) power coefficient Cp, (c) pitch angleβ and (d) speed ratio λ

The coefficient Cp correctly follows its reference, stabilizing at the value of 0.48. The same thing for the speed ratio λ, which takes the value of 8 in static conditions. The setting angle β is set to zero, in order to extract the maximum power from the wind.

3.3. Maximum power point tracking with speed control

The power captured by the wind turbine can be maximized by adjusting the *Cp* coefficient. This coefficient is dependent on the speed of the generator. Using a variable speed wind turbine maximizes this power. The control algorithm without speed regulation is illustrated in Figure 4 [22], [23]. In this work, we discuss the development of the DFIG oriented stator flux vector control, the flux will on axis (d) and stator voltage on axis (q). Thus, we obtain a decoupled linear model [24].

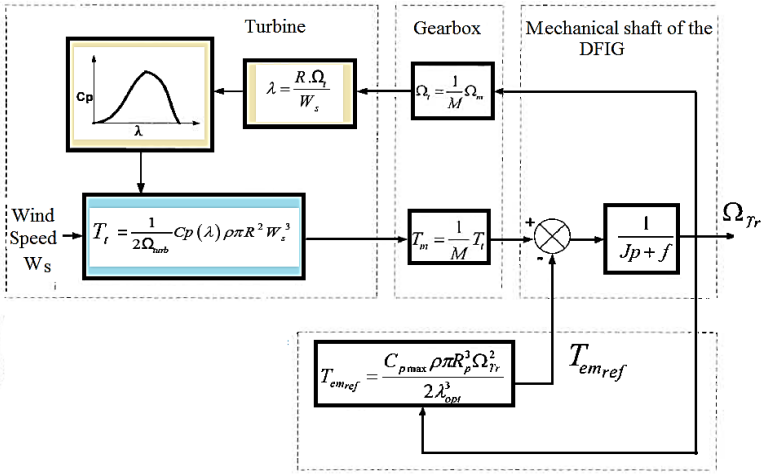

Figure 4. MPPT control without speed control

4. DFIG MODELING AND CONTROL

We can write:

$$\emptyset_{ds} = \emptyset_s \; ; \; \emptyset_{qs} = 0 \tag{4}$$

The power equations according to the previously considered hypotheses become as follows:

$$P_s = -\frac{V_s M}{L_s} i_{qr} \tag{5}$$

$$Q_s = \frac{V_s^2}{\omega_s L_s} - \frac{V_s M}{L_s} i_{dr} \tag{6}$$

It emerges from (5) and (6) that the control of the active and reactive powers at the stator is decoupled. The active stator power produced by the machine is controlled by the i_{qr} component.

Whereas, the reactive power is controlled by the component i_{dr}, eventually controlled at zero to obtain a unitary power factor at the stator. The rotor voltages, which are the outputs of the current controllers, are given by [25].

$$V_{dr} = R_r i_{dr} + \left(L_r - \frac{M^2}{L_s}\right)\frac{d i_{dr}}{dt} - g\omega_s \left(L_r - \frac{M^2}{L_s}\right) i_{qr} \tag{7}$$

$$V_{qr} = R_r i_{qr} + \left(L_r - \frac{M^2}{L_s}\right)\frac{d i_{qr}}{dt} + g\omega_s \left(L_r - \frac{M^2}{L_s}\right) i_{dr} + g\omega_s \frac{V_s M}{\omega_s L_s} \tag{8}$$

The block diagram of the DFIG electrical system, fit to the regulation and control of powers (*P*, *Q*), is shown in Figure 5. The Indirect control goes through two important steps, the first consists of calculating the reference currents from the set points of the active and reactive powers in a closed loop, the second calculates the reference voltages (V_{dr_ref} and V_{qr_ref}) from the rotor currents calculated by the first subsystem, as shown in Figure 5. The block contains on each axis, two types of classical *PI* regulator, axis of active powers: (*Kpq* = 50, *Kiq* = 70000, *Kpq* = 1, *Kiq* = 1500) and the other of reactive powers: (*Kpd* = 50,

Kid = 70000, *Kpd* = 1, *Kid* = 1500). The first regulator designed to control the powers while the second is to regulate the rotor currents.

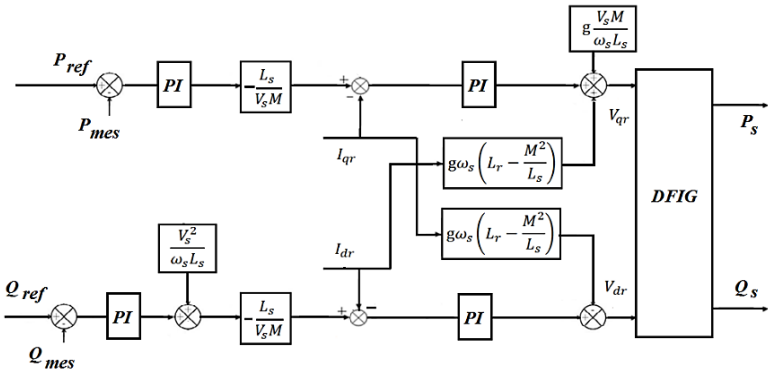

Figure 5. Block diagram of the indirect control of the DFIG

5. MODEL OF FIVE LEVEL PMW INVERTER

5.1. Five level inverter modeling

The MPC structure of the three-phase five-level inverter is shown in Figure 6. The complementary control retained [26], [27] is characterized by a relationship between the connection functions of the switches of an arm k as follows (9):

$$F'_{ki} = 1 - F_{k(5-i)}\,, i = 1, \ldots\ ,4\,;\ \ k = 1, 2, 3 \tag{9}$$

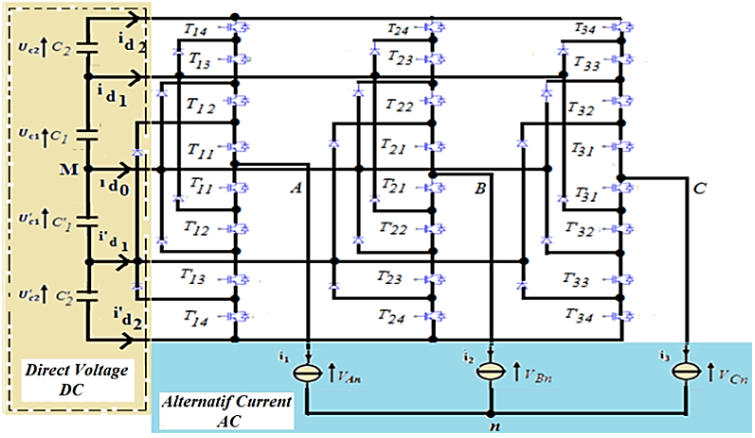

Figure 6. Five level inverter MPC Structure

The output voltages v_{kn} of the inverter are expressed according to the system (10), as follows:

$$\begin{bmatrix} v_{1n} \\ v_{2n} \\ v_{3n} \end{bmatrix} = \frac{1}{3}\begin{bmatrix} 2 & -1 & -1 \\ -1 & 2 & -1 \\ -1 & -1 & 2 \end{bmatrix}\left\{\begin{pmatrix} F_1^b + F_1^{b1} \\ F_2^b + F_2^{b1} \\ F_3^b + F_3^{b1} \end{pmatrix} U_{C1} + \begin{pmatrix} F_1^b \\ F_2^b \\ F_3^b \end{pmatrix} U_{C2} - \begin{pmatrix} F_1'^b + F_1'^{b1} \\ F_2'^b + F_2'^{b1} \\ F_3'^b + F_3'^{b1} \end{pmatrix} U'_{C1} + \begin{pmatrix} F_1'^b \\ F_2'^b \\ F_3'^b \end{pmatrix} U'_{C2}\right\} \tag{10}$$

Knowing that:

$$\begin{cases} F_k^b = F_{k1}F_{k2}F_{k3}F_{k4} \\ F_k'^b = F'_{k1}F'_{k2}F'_{k3}F'_{k4} \\ F_k^{b1} = F_{k1}F_{k2}F_{k3}(1 - F_{k4}) \\ F_k'^{b1} = F'_{k1}F'_{k2}F'_{k3}(1 - F'_{k4}) \end{cases} \tag{11}$$

5.2. Strategy control of a five-level inverter

The inverter is controlled by the sinusoidal pulse width modulation (SPWM) strategy [28]–[30]. The control signals of an inverter arm are determined by comparing the four carriers with three sin wave reference shown in Figure 7. This technique is characterized by the modulation index (m) and modulation rate (r). The control algorithm of the switches of the first arm of the inverter at five levels is illustrated in Figure 8. The results of simulations obtained during the implementation of the three-phase inverter with five levels in open loop (for V_{dc}=1600V, r=0.8 and m=18), clearly show the five levels of the voltage V_{aM}, illustrated in the Figure 9, as well as the voltage of the first phase Van and its fundamental as illustrated in Figure 10.

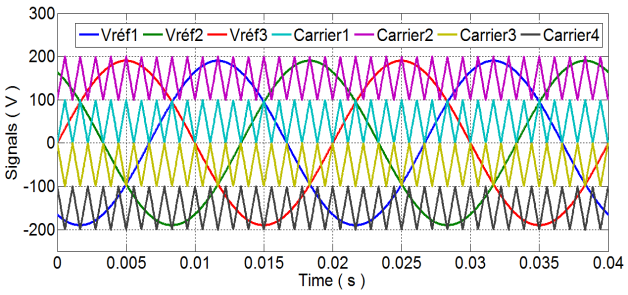

Figure 7. Strategy phase opposition disposition (POD) SPWM five levels inverter four carriers (m=18, r =0.8)

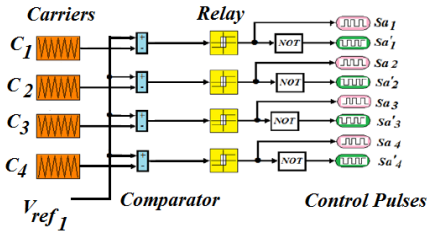

Figure 8. Control algorithm PWM five levels inverter (for phase 1)

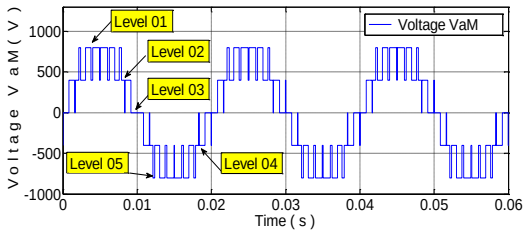

Figure 9. Output voltage V_{aM} of the five-level inverter (m=18, r=0.8, V_{dc}=1600 V)

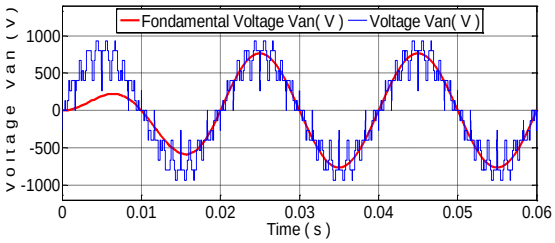

Figure 10. Voltage and fundamental voltage Van of the five-level inverter (m=18, r=0.8, V_{dc}=1600V)

6. RESULTS AND DISCUSSION

The parameters of DFIG used in the energy conversion are [21]: 4 kW, 220/38 0V, 50 Hz, 15/8.6 A, 1440 rpm; Moment of inertia: J=0.2 kg.m²; Viscous coefficient of friction: f=0.001 N.m.s/rd. The DFIG, is driven by the wind turbine, at a wind speed of 8 m/s. Controlled by the oriented stator flux indirect vector control (IFOC), whose active and reactive powers are decoupled.

6.1. The rotor of the DFIG is supplied by two-level inverter

The results obtained in Figure 11, Figure 12 and Figure 13, show that the variation of the electrical power is adapted to the variation of the speed of the DFIG, the latter is adapted to the variation of the wind speed. This shows the influence of the variation of the mechanical speed according to the wind speed on the electrical power. The speed and mechanical torque of the turbine are shown in Figure11 (a) and Figure 11(b), respectively. On the other hand, the Figure 12(a) and Figure 12(b) respectively represent the speed of rotation and the mechanical torque of the doubly fed induction generator (DFIG). Figure 13(a) and Figure 13(b) respectively show that there is also good monitoring of the active power set point as well as of the reactive power, generated by the doubly fed induction generator. The latter is maintained at zero in order to ensure a unity power factor on the stator side, so as to optimize the quality of the energy returned to the network.

Figure 14 and Figure 15, show respectively the stator and rotor current of the first phase, where the good sinusoidal alternating shape is observed. Figure 16(a) shows the rotor voltage produced by the two-level inverter powered by a DC voltage bus of V_{dc}=650 V, of which fp=5 kHz and r=0.8. This voltage has a harmonic distortion rate of 10.3% for a simulation time of 0.1 second, as shown in Figure 16(b). The total harmonic distortion of the current (67%) at the rotor in Figure 17 is very far from international standards, which require a rate of less than 5%. This is mainly due to the lack of a filtering mean on one hand, the

drawbacks of PWM modulation with natural sampling and the topology of the inverter on the other hand. On the other hand, the stator current in Figure 18 has a very acceptable THD (1.26%), because it presents almost sinusoidal shapes as shown in Figure 14. It is pointed out here that the rotor current following the d-q mark (I_{rd} and I_{rq}) correctly follows the law of the indirect control of the active and reactive powers of the DFIG. Since we can clearly see that the current I_{dr} depends on the reactive power by taking the same shape of Q_{ref}, then the current I_{rq}, depends on the active power by taking the shape of P_{ref} shown in Figure 19(a) and Figure 19(b) respectively.

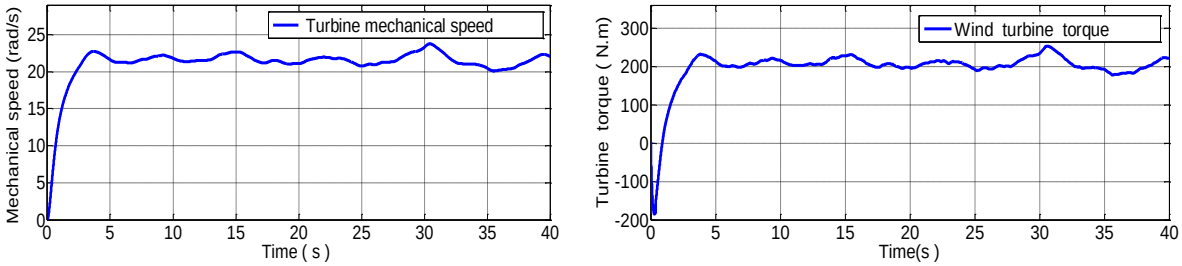

(a) (b)

Figure 11. Turbine mechanical (a) speed and (b) torque

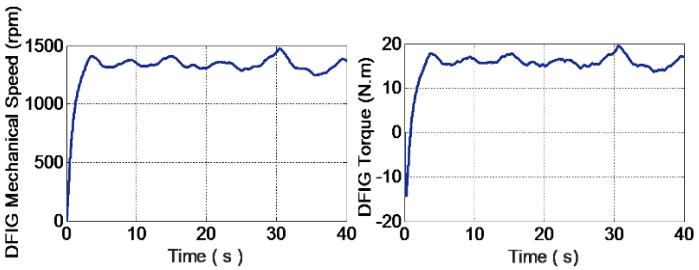

(a) (b)

Figure 12. DFIG mechanical (a) speed in rpm and (b) torque in N.m

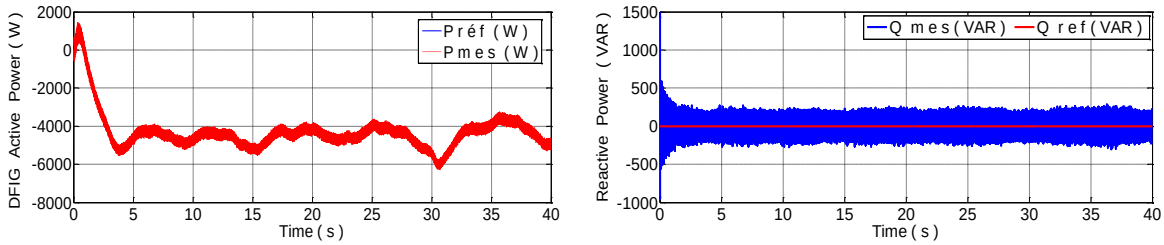

(a) (b)

Figure 13. DFIG (a) active power and (b) reactive power

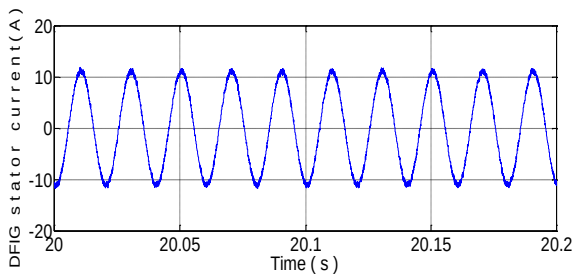

Figure 14. Zoom of the current of the first stator phase

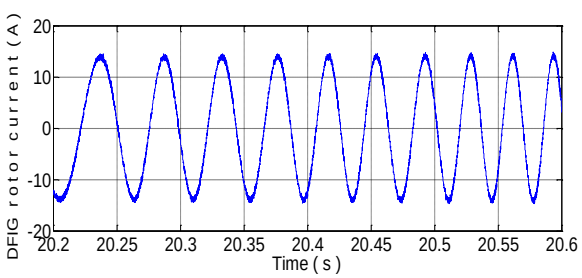

Figure 15. Zoom of the current of the first rotor phase

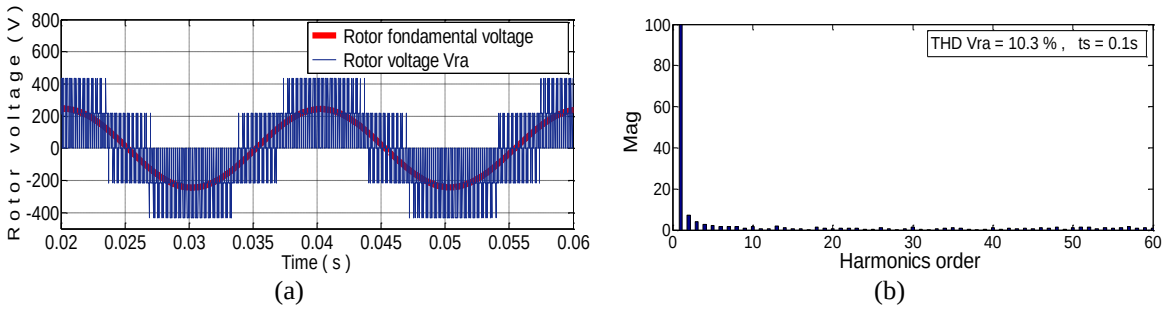

Figure 16. Zoom voltage of the first phase rotor (a) by a two-level inverter and (b) its harmonic distortion

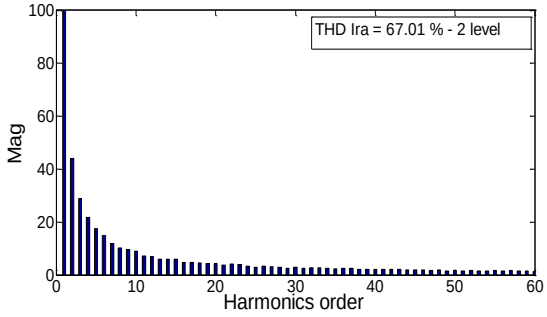

Figure 17. Harmonic distortion total of the rotor current delivered by a two-level inverter

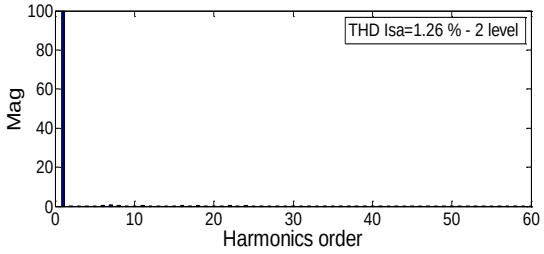

Figure 18. THD of the stator current when a two-level inverter supplies the rotor

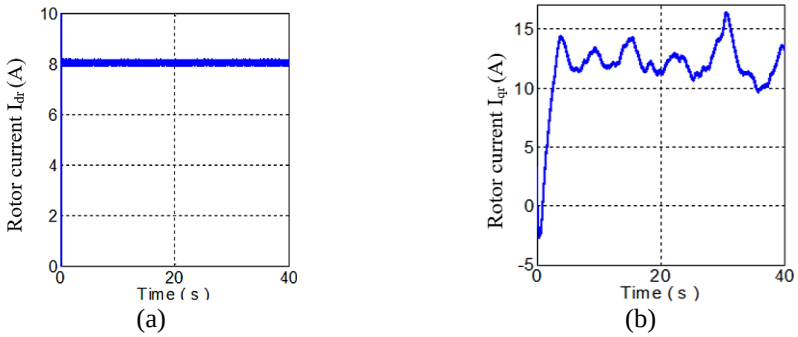

Figure 19. DFIG rotor currents I_{dr} (a) and (b) I_{qr}, supplied by a two-level inverter

6.2. The rotor of the DFIG is supplied by a five-level inverter

It in this case, the rotor is supplied by an inverter with five voltage levels, the latter is supplied by a direct voltage bus V_{dc}= 650 V, controlled by the multi-level PWM technique (f_p=5 kHz, r=0.8 at four carriers). What should be noted from the results obtained during the simulation is that all the quantities, namely: speed, torques, powers and stator currents have the same appearance as the quantities obtained above, when the rotor is powered by a two-level inverter. With the exception of the rotor voltage, which contains five voltage levels (V_{aM}, V_{bM}, V_{cM}, visualized in Figure 20), which gives a phase voltage V_{ra}, approaching a sinusoid, the case of Figure 21(a). While presenting a harmonic distortion rate (THD V_{ra}) of 9.85%, mentioned in Figure 21(b), for a simulation time of 0.1 seconds, lower than that obtained by a two-level inverter (10.3% of Figure 16(b)).

The same goes for the rotor current Ira of the first phase, delivered by the five-level inverter, mentioned in Figure 22(a), it has a distinctly sinusoidal shape with a THD equal to 7.45% as shown in Figure 22(b), of better quality compared to that obtained by a two-level inverter (THD I_{ra}=67%, of Figure 17).The current form at the stator Isa gets improved much more when the rotor is supplied by a five-level inverter (*THD Isa*=0.0978%, Figure 23), comparing it to the two-level one (THD I_{sa}=1.26%, Figure 18).The Table 1 summarizes the rate of distortion of the rotor and stator quantities, depending on the structure of the inverter which supplied the circuit of the rotor

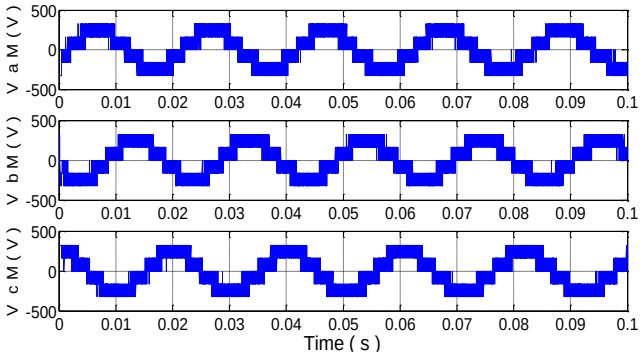

Figure 20. Voltages of the three arms of the five-level inverter (between phase and reference point M)

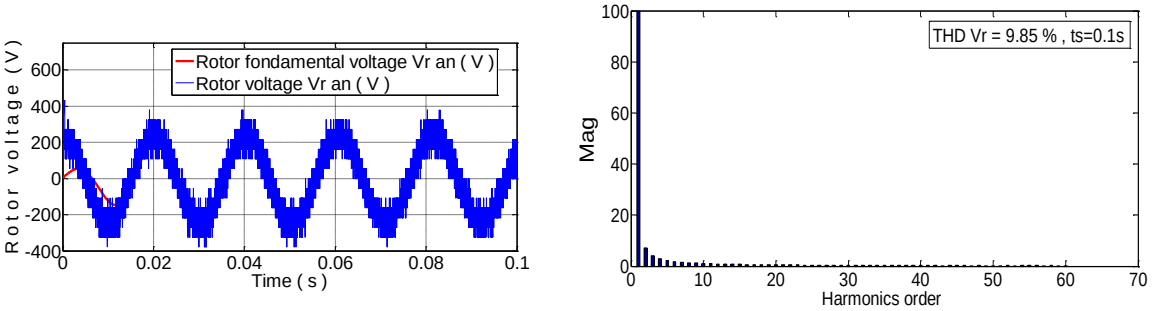

(a) (b)

Figure 21. Rotor voltage delivered by (a) a five-level inverter and (b) its harmonic spectrum

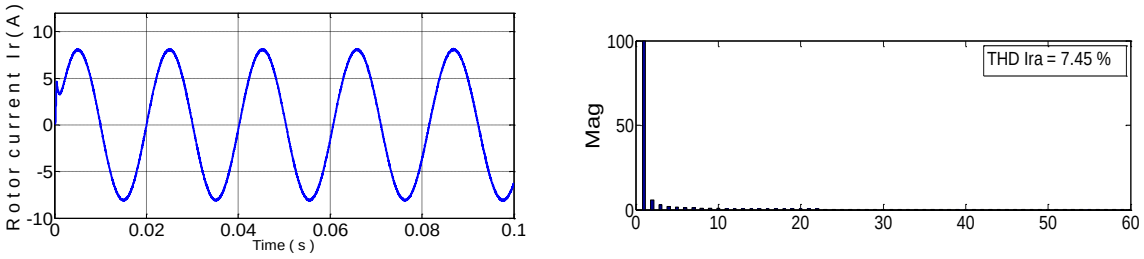

(a) (b)

Figure 22. Rotor current delivered by (a) a five-level inverter and (b) its harmonic spectrum

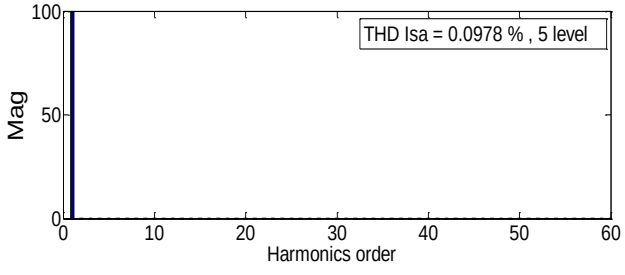

Figure 23. THD of the stator current when a five-level inverter supplies the rotor

Table 1. Currents/voltages THD for converters with two and five levels

Power supply to the rotor	$THDV_{ra}$(%)	$THDI_{ra}$(%)	$THDI_{sa}$(%)
Two-level inverter	10.3	67	1.26
Five-level inverter	09.85	07.45	0.0978

7. CONCLUSION

We have developed in this article the method of indirect control in active and reactive power at the stator of the DFIG, in a wind energy conversion system based on a PWM inverter with two then with five levels. The results show that the indirect vector control (IFOC) developed, using control algorithms associated with PI regulators, makes it possible to obtain good decoupling of the powers at the stator of the machine, with good monitoring of the values of reference, where the reactive power is kept zero at the moment when the DFIG machine produces active power on the electrical network. The static inverters used in the rotor circuit of the DFIG (inverter with two then five levels), controlled by the PWM technique, gave satisfaction for their contributions to the decoupling of the powers and the correct operation of the DFIG. The five-level inverter responds well by giving better harmonic distortion rates of currents to the rotor and stator of the DFIG, compared to the two-level inverter. The five-level inverter therefore offers the possibility of reducing the THD of the electrical signals in the absence of a filtering device.

Therefore, as a valuation of the research results, considering the large number of switches per arm of the five-level inverter, the possibility of the latter to increase the DC bus voltage and thus overcome the obstacle the maximum reverse voltage of each switch. This means, as prospects, the possibility of increasing the power supplied to the electrical network within the limits where the currents do not take unacceptable values in the coils of the machine. The conversion of wind energy based on multi-level inverters is entirely possible in the field of high powers and high voltages, with good quality electrical energy.

REFERENCES

[1] A. Mirecki, "Comparative study of energy conversion chains dedicated to a small power wind turbine," Ph.D. dissertation, Dept. Elect. Eng., National Polytechnic Institute, Toulouse, French, 2005. [Online]. Available: https://inis.iaea.org/collection/NCLCollectionStore/_Public/37/038/37038440.pdf?r=1

[2] A. Dendouga, "Control of the active and reactive power of the double-fed asynchronous machine (DFIM)," Ph.D. dissertation, Dept. Elect. Eng., Batna Univ., Algeria, 2010.

[3] Y. Djeriri, "Vector control of a DFIG integrated into a wind power system," Ph.D. dissertation, Dept. Elect. Eng., Djillali Liabes Univ., Algeria, 2009.

[4] M. Hacil, "Improving wind energy performances," Ph.D. dissertation, Dept. Elect. Eng., Constantine Univ., Algeria, 2012.

[5] A Lilia, "Contribution to improving the performances of wind generators," Ph.D. dissertation, Dept. Elect. Eng., Batna Hadj Lakhdar Univ., Algeria, 2012.

[6] S.Nemsi, "Study and control of a MADA with storage Application to a distribution network," Ph.D. dissertation, Dept. Elect. Eng., Houari Boumediene Univ., Algeria, 2011.

[7] S.EL Aimani, "Modeling of different wind turbine technologies integrated in a medium voltage network," Ph.D. dissertation, Dept. Elect. Eng., School central of Lille (ECL), French, 2005.

[8] A. Boyette, "Control-command of a dual power asynchronous generator with a storage system for wind power generation," Ph.D. dissertation, Dept. Elect. Eng., Henri Poincaré Univ., Nancy 1, French, 2006.

[9] F. Poitiers, "Study and control of asynchronous generators for the use of wind power, asynchronous machine with stand-alone cage, Asynchronous machine with double power supply connected to the network," Ph.D. dissertation, Dept. Elect. Eng., Nantes Univ., French, 2003.

[10] S. Mondai, and D. Kastha, "Improved direct torque and reactive power control of a matrix-converter-fed grid-connected doubly fed induction generator," *IEEE Transactions On Industrial Electronics*, vol. 62, no. 12, pp. 7590–7598, December 2015, doi:10.1109/TIE.2015.2459056.

[11] D. Lecocq, P. Lataire, and W. Wymeersch, "Application pf the doubly fed asynchronous motor (DFAM) in variable speed drive," *EPE association*, Bughton, September 1993, pp. 419–423.

[12] F. Blaschke, "The principle of field oriented as applied to the new tran vector closed-loop control system for rotating machine," *Siemens Review*, vol.39, no. 4, pp. 217–220, 1972.

[13] W. Leonhard, "Control of AG-machines with the help of microelectronics," *IFAC Proceedings Volumes*, vol. 16, no. 16, September 1983, pp. 35–58, doi: 10.1016/S1474-6670(17)61941-4.

[14] J. C. F. Soltoski, P. T. P. dos Santos, and C. H. I. Font, "Development of a small scale wind turbine emulator work bench," *12th IEEE International Conference on Industry Applications* (INDUSCON), November 2016, pp. 1–8, doi:10.1109/INDUSCON.2016.7874577.

[15] A. Rahab, F. Senani, and H. Benalla, "Direct power control of brushless doubly-fed induction generator used in wind energy conversion system," *International Journal of Power Electronics and Drive System (IJPEDS)*, vol. 8, no. 1, pp. 417–433, March 2017.

[16] B. Hamane, M. L. Doumbia, M. Bouhamida, and M. Benghanem, "Control of wind turbine based on DFIG using Fuzzy-PI and Sliding Mode controllers," *Ninth International Conference on Ecological Vehicles and Renewable Energies (EVER),IEEE Xplore*, March 2014, pp. 1–8, doi:10.1109/EVER.2014.6844060.

[17] S. Kouadria, E. M. Berkouk, Y. Messlem, and M. Denaï, "Improved control strategy of DFIG-based wind turbines using direct torque and direct power control techniques," *J. Renew. Sustain. Energy*, vol. 10, no. 4, pp. 304–306, 2018, doi:10.1063/1.5023739.

[18] Belkacem, N. Bouhamri, L. A. Koridak, and A. Allali, "Fuzzy optimization strategy of the maximum power point tracking for a variable wind speed system," *International Journal of Electrical and Computer Engineering (IJECE)*, vol. 12, no. 4, pp. 4264–4275, August 2022, doi: 10.11591/ijece.v12i4.pp4264-4275.

[19] M. El Azzaoui, H. Mahmoudi, B. Bossoufi, and M. El Ghamrasni, "Emulation of wind conversion chain equipped with a doubly fed induction generator," *International Symposium on Fundamentals of Electrical Engineering(ISFEE)*, 2016, pp. 1–6, doi:10.1109/ISFEE.2016.7803155.

[20] D. Ochoa and S. Martinez, "A simplified electro-mechanical model of a DFIG-based wind turbine for primary frequency control studies," *IEEE Lat. Am. Trans*., vol. 14, no. 8, pp. 3614–3620, 2016,doi:10.1109/TLA.2016.7786341.

[21] Y.A. Bencherif, "Modeling and control of a dual power asynchronous machine for the production of wind energy," Master, National Polytechnic School, Dept. Elect. Eng., June 2008, Algeria.

[22] Hamzaoui,F. Bouchafaa, A. Hadjammar, and A. Talha, "Improvement of the performances MPPT system of wind generation,"*Electronics, Communications and Photonics Conference (SIECPC)*, Saudi International, April 2011, pp. 1–6, doi:10.1109/SIECPC.2011.5876886.
[23] A. M. Sylla, and M. L. Doumbia, "Maximum power control of grid-connected DFIG-based wind systems," *IEEE Electrical Power & Energy Conference (EPEC)*, London, ON, Canada, October 2012, doi:10.1109/EPEC.2012.6474963.
[24] N. K. Swami Naidu and B. Singh, "Experimental implementation of doubly fed induction generator-based standalone wind energy conversion system," *IEEE Trans. Ind. Appl*., vol. 52, no. 4, pp. 3332–3339, Jul 2016, doi:10.1109/TIA.2016.2542783.
[25] D. Zhu, X. Zou, L. Deng, Q. Huang, S. Zhou, and Y. Kang, "Inductance-emulating control for DFIG-based wind turbine to ride-through grid faults,"*IEEE Trans. Power Electron*., vol. 32, no. 11, pp. 8514–8525,Nov 2017, doi:10.1109/TPEL.2016.2645791.
[26] D. Lalili, N. Lourci, E.M. Berkouk, F.Boudjema, J.Petsoldt, and M.Y.Dali, "A simplified space vector pulse width modulation algorithm for five-level diode clamping inverter," *International Symposium on Power Electronics, Electrical Drives, Automation and Motion, SPEEDAM06*, May 2006, pp. 1349–1354, doi:10.1109/SPEEDAM.2006.1649977.
[27] M. M. Tounsi, A. Allali, H. M. Boulouiha, and M. Denaï, "ANFIS control of a shunt active filter based with a five-level NPC inverter to improve power quality," *International Journal of Electrical and Computer Engineering (IJECE)*, vol. 11, no. 3, pp. 1886–1893, 2021, doi: 10.11591/ijece.v11i3.pp1886-1893.
[28] M. S. Djebbar and H. Benalla, "The high performances of a seven levels active power filter with a fuzzy logic controller under a high voltage," *Journal of Engineering Science and Technology*, vol. 13, no. 5, pp. 1315–1329, May 2018.
[29] N. Prabaharan and K. Palanisamy, "Comparative analysis of symmetric and asymmetric reduced switch PWM topologies using unipolar pulse width modulation strategies," *IET Power Electronics*, vol. 9, no. 15, pp. 2808–2823, December 2016, doi:10.1049/iet-pel.2016.0283.
[30] V.-Q. Nguyen and Q.-T. Tran, "Reduction of common mode voltage for cascaded multilevel inverters using phase shift keying technique," *Indonesian Journal of Electrical Engineering and Computer Science*, vol. 21, no. 2, pp. 691–706, June 2021, doi: 10.11591/ijeecs.v21.i2.pp691-706.

BIOGRAPHIES OF AUTHORS

Mohamed Salah Djebbar was Professor of Electrical Engineering from 1989 to 2009 at the technical school of Constantine, Algeria. Obtained a degree in electrical engineering from the University of Annaba/Algeria in 1989; then magister degree in control of electrical machines in 2005. He received the Ph.D. degree from the Electrical Engineering, Constantine University, Algeria in 2017. Currently, he is a professor at the Larbi Tebessi University of Tébessa, Algeria in electrical engineering department. The research work is related to the field of static converters, the quality of electrical energy, electrical machines and drives. He can be contacted by email: djebbarcn@yahoo.fr.

Aziz Boukadoum was born in Constantine, Algeria; He received the Ph.D. degree from the Electrical Engineering, Annaba University, Algeria in 2015. Currently, he is a professor in Larbi Tebessi university, Tebessa of Electrical Engineering Institute, Algeria. His research interests include power quality, electrical machines and drives, faults diagnosis and artificial intelligent. He can be contacted at email: azizboukadoum@yahoo.fr.

Abla Bouguerne was born in Skikda, Algeria; He received the Ph.D. degree from the Electrical Engineering, Constantine University, Algeria in 2017. Currently, he is a professor in Larbi Tebessi university, Tebessa of Electrical Engineering Institute, Algeria. His research interests include diagnosis of induction machine faults and artificial intelligent. She can be contacted at email: bouguerneabla@yahoo.fr.